JET–R(98)06

S A Arshad et al

Measurement of Photomultiplier Effective Quantum Efficiency

JET–R(98)06

Measurement of Photomultiplier Effective Quantum Efficiency

S A Arshad, C W Gowers, P Nielsen.

JET Joint Undertaking, Abingdon, Oxfordshire, OX14 3EA.

July 1998

INTRODUCTION

The JET divertor LIDAR system, KE9D, is being modified to perform measurements of plasma edge electron temperature and density in the new gas-box divertor configuration. The change involves raising the line of sight from the divertor region so that the laser beam passes through the plasma edge reaching a depth of ~5cm inside the boundary. Changes are also being made to the detection system. This currently employs a grating spectrometer and a streak camera. The new system will contain a 4-channel filter spectrometer with microchannel plate (MCP) photomultipliers. There are several advantages of these changes:

- The detector area is larger, providing a larger detector image in the plasma. This allows a wider vignetting curve, increasing the spatial coverage of the system.
- The spectrum of the edge plasma is often too broad for the existing system. The new system will provide increased spectral coverage, and thereby a higher T_e capability.
- The reflection of the laser beam from the inner wall is too bright for the streak camera and corrupts the data in the present system, including the plasma data preceding the reflection. This difficulty is removed with the photomultipliers.
- In contrast to the streak camera the data acquisition from photomultipliers can be easily extended to make an accurate measurement of the plasma background emission levels which need to be subtracted before the true scattering signal is obtained.

An important parameter determining the quality of the signal from a photomultiplier is its effective quantum efficiency, calculated from the observed signal and noise characteristics. This parameter has been measured at JET for three commercial photomultipliers with a view to selecting a detector for the new KE9D system. The measurement is described in this paper and results for the three detectors are given.

The spatial resolution for a LIDAR system is given by

$$\Delta L = c/2(\tau^2_{laser} + \tau^2_{det})^{1/2},$$

where c is the velocity of light, τ_{laser} is the laser pulse duration (300ps for the KE9D laser), and τ_{det} is the detection response time, including the contribution from the digitiser. With the streak camera the potential spatial resolution is ~9cm, whereas for the three photomultipliers response time measurements show that spatial resolutions of 9cm, 10cm and 12cm are possible with the Photek, Hamamatsu and ITT detectors respectively. A resolution of 12cm along the laser line is still within the range of interest for the KE9D edge measurement, although better resolution would be advantageous.

Figure 1 shows a schematic of a microchannel plate photomultiplier. The photoelectrons are multiplied in the microchannels producing a voltage at the output proportional to the number of photoelectrons. Steady illumination of the detector produces a mean output level

$$S = e\nu nqTR,$$

where q is the photocathode quantum efficiency, e is the electron charge, ν is the electron multiplication factor, n is the photon arrival rate at the detector, T is the transmission coefficient, representing the fraction of photoelectrons that are collected for multiplication, and R is the resistance at the anode (see Figure 1).

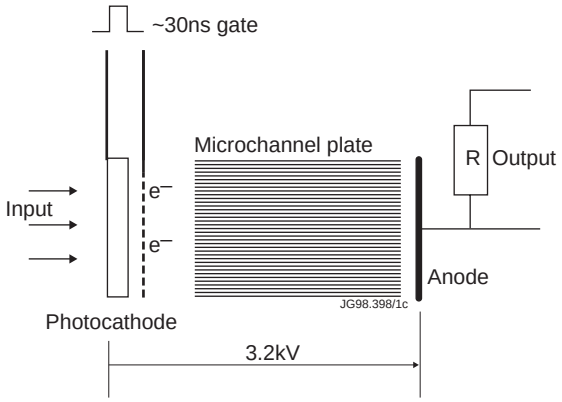

Figure 1: Example of a microchannel plate photomultiplier

In the case of an ideal detector amplification noise arises purely from photon statistics. The standard deviation of the signal $N_{ph.\ rms}$ is then related to the photon flux by

$$\tau N_{ph.\ rms} = e\nu(nqT\tau)^{1/2}R,$$

where $\tau = (\pi/2)^{1/2}\ \tau_{AC}$ is the characteristic time of the system, τ_{AC} being the width of the autocorrelation function of the noise (signal - mean). From these expressions it follows that

$$qT = (S/\ N_{ph.\ rms})^2/n\tau.$$

In general there may be significant contributions to the measured noise from sources other than photon statistics. For this case the effective quantum efficiency is defined following the above expression

$$q_{eff.} \equiv (S/\ N_{rms})^2/n\tau,$$

which is the more interesting parameter for characterising the overall performance of the detector. The detector gain ν is also quoted by the manufacturer and this allows qT to be evaluated from

$$q = S\ /\ e\nu nTR.$$

METHOD

The set-up for making the measurement is shown Figure 2. The power output of the 670nm laser on the right was measured with a diode detector, so that the source photon flux is known. The lens broadens the laser beam to produce a spot size on the detector corresponding to that in the real KE9D measurement. The attenuation consists of neutral density filters, to reduce and scan the power input in the range 0.1-1μW. The high voltage supply provides variable voltage in the kV range allowing the gain of the detector to be varied.

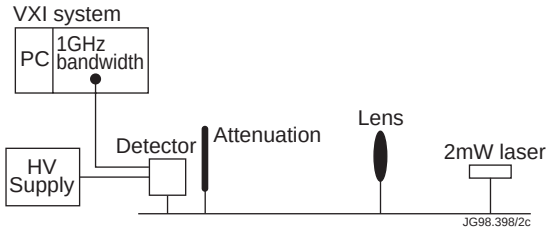

Figure 2: Arrangement for measurement of quantum efficiency

At each high-voltage setting and attenuation level 100 traces of duration 50ns each were recorded at 5GHz sampling (1GHz bandwidth). The detector was gated on for several tens of nanoseconds during each observation. The mean signal level and standard deviation were calculated from each set of 100 traces. The system response time was evaluated from the average of the autocorrelation functions of the set of 100 traces. This procedure was repeated for three detectors.

RESULTS

Figure 3 shows the overlay of 10 traces of the raw signal from the Hamamatsu detector at maximum gain and power input of ~1μW. By averaging 100 such traces the mean signal level is obtained, and the dependence of this on power input for the three tubes is shown in Figure 4. The straight lines show the linearity of the detectors over the power range. Similarly the standard deviation N_{rms} of the data was calculated from 100 traces at each power level and is plotted in Figure 5. The linear dependence of N_{rms} on the square root of the power input over the range shows that the noise indeed scales in the expected way for Gaussian statistics. The results for the three detectors at maximum gain are summarised in Table 1.

Detector	$(S/N_{rms})^2$	τ_{AC} [ns]	Input [ph/ns]	q [%]	qT [%] (from quoted gain)	qeff [%]
Hamamatsu	19	0.7	3347	7	7	**0.66**
Photek	14	0.62	3347	5.5	4	**0.53**
ITT	49	0.9	3107	5.2	2	**1.39**

Table 1: Comparison of the three photomultipliers at maximum gain

ESTIMATE OF THE AMPLIFICATION NOISE FACTOR

The electron amplification in the MCP is a statistical process involving a varying number of bounces in the channels (10-20), each bounce with a relatively low secondary electron emission coefficient. The probability function of the gain even for a double MCP is very broad. The mean amplifications for the three tubes are from 10^5 to 5×10^5. The measured pulse height distribution is given in the data sheet for the Hamamatsu tube. We assume the general characteristics to be the same for the other tubes.

Using the Hamamatsu data we have simulated the measured signals and the increased noise resulting from the amplification. Comparing the rms noise in simulations with and without added noise we find a noise factor of F~1.2. This surprisingly small increase in the noise can be easily demonstrated by repeatedly calculating the signal resulting from e.g. 100 events. The resulting histogram is a Gaussian distribution with a standard deviation of ~6, i.e. a noise factor F~1.2. Changing the number of events we find that the noise increases as $N^{1/2}$.

CONCLUSIONS

The effective quantum efficiencies of the three tubes are all well below the measured quantum efficiency of the photocathode. We do not know the exact reason for this large drop. The noise resulting from the amplification process seems to play only a minor role. We can guess on other factors influencing the performance of the MCP photomultipliers. The packing fraction of the microchannels is an obvious loss accounting for about 30%. Various films / coatings over both the photocathode and over the front end of the MCP will diminish the transmission of photoelectrons to the MCP. These films are applied to increase the gating speed of the tubes and to protect against damage from sputtering. The Hamamatsu tube in addition has a gating grid with a quoted transmission of 70%.

High effective quantum efficiency is imperative in our application. The faster response time of the Hamamatsu and Photek tubes relative to the ITT tube does not make up for their much lower q_{eff}. The resulting gradient scale-length that can be measured with these tubes would not be better than the ITT tube due to a larger uncertainty of the measured electron temperature / density at a given point. We have therefore decided to initially use the ITT MCP photomultipliers in the upgraded KE9D.

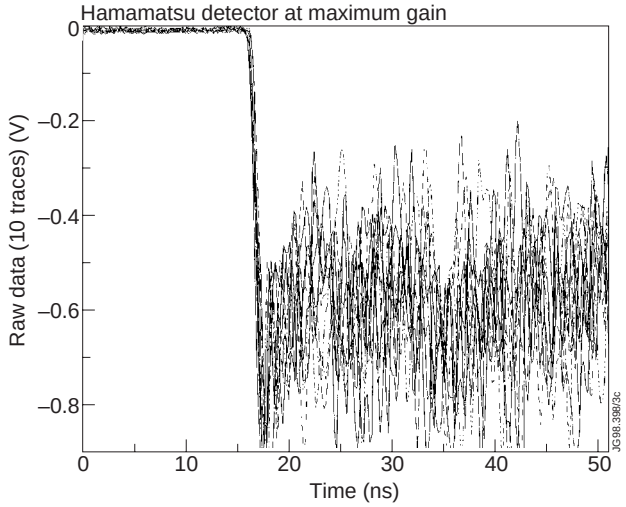

Figure 3: Example raw data for the Hamamatsu detector, showing an overlay of 10 traces. The detector is gated on ~16ns after the start of data acquisition, and until the end of acquisition.

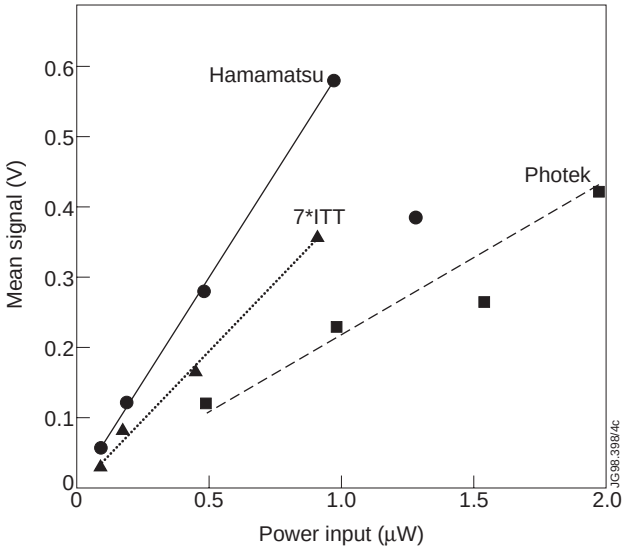

Figure 4: Mean signal levels for the 3 detectors at maximum gain

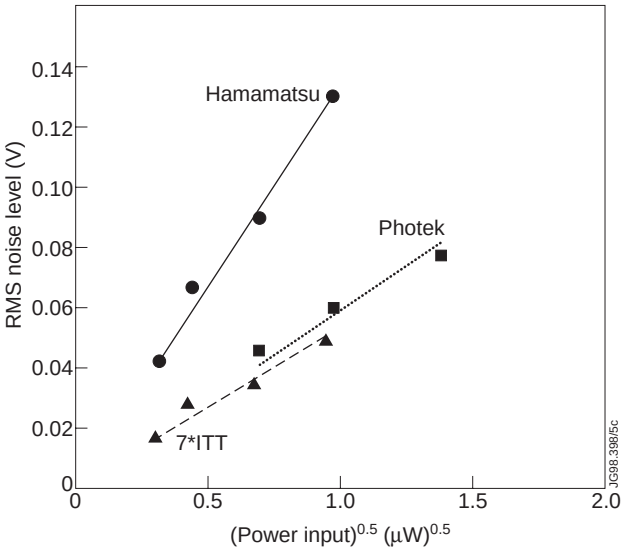

Figure 5: Noise characteristics for the 3 detectors at maximum gain